

**Figure 1** Analysis of  $\text{Mg}^{2+}$  speciation in *E. coli* metabolite mixtures. Eco80 contains **(A)** *E. coli* metabolome molar composition. Eco80 contains the 15 most abundant metabolites that compose 80% of the *E. coli* metabolome. NTPCM contains four strong  $\text{Mg}^{2+}$  chelating NTPs, and WMCM contains 11 other weak  $\text{Mg}^{2+}$  binding metabolites **(B-D)** Effect of  $\text{Mg}^{2+}$  on 8-hydroxyquinoline-5-sulphonic acid (HQS) emission with and without mixtures of metabolites that chelate  $\text{Mg}^{2+}$ . Grey lines represent fits to determine the binding constant for  $\text{Mg}^{2+}$  and HQS. **(E-G)** Effect of the total  $\text{Mg}^{2+}$  concentration on the free  $\text{Mg}^{2+}$  concentration with mixtures of metabolites that chelate  $\text{Mg}^{2+}$ . Free  $\text{Mg}^{2+}$  was calculated using HQS emission and the binding constant for  $\text{Mg}^{2+}$  and HQS. Grey lines represent the free  $\text{Mg}^{2+}$  concentration in the absence of chelators (free  $\text{Mg}^{2+}$  = total  $\text{Mg}^{2+}$ ). Hex bins represent a statistical simulation of 1000 virtual artificial cytoplasms based on experimental errors in  $K_D$  determination, experimental errors in reagent concentrations, and single site binding.

**Table 1.** Eco80: the top 15 most abundant metabolites that comprise 80% of the *E. coli* metabolome.

Metabolite	Conc. (mM)	K <sub>D</sub> (mM)	Chelation strength
ATP	9.63	0.28 (0.01) <sup>a</sup>	NTPCM (Strong <sup>d</sup> )
UTP	8.29	0.248 (0.004) <sup>a</sup>	NTPCM (Strong <sup>d</sup> )
GTP	4.87	0.201 (0.007) <sup>a</sup>	NTPCM (Strong <sup>d</sup> )
dTTP	4.62	0.160 (0.003) <sup>a</sup>	NTPCM (Strong <sup>d</sup> )
L-Glutamic acid	96	520 (50) <sup>b</sup>	WMCM (Weak <sup>d</sup> )
Glutathione	16.6	NA <sup>c</sup>	WMCM (Weak <sup>d</sup> )
Fructose 1,6- biphosphate	15.2	5.9 (0.1) <sup>a</sup>	WMCM (Weak <sup>d</sup> )
UDP-N- acetylglucosamine	9.24	29 (2) <sup>a</sup>	WMCM (Weak <sup>d</sup> )
Glucose 6-phosphate	7.88	17.3 (0.2) <sup>a</sup>	WMCM (Weak <sup>d</sup> )
L-Aspartic acid	4.23	465 (12) <sup>b</sup>	WMCM (Weak <sup>d</sup> )
L-Valine	4.02	NA <sup>c</sup>	WMCM (Weak <sup>d</sup> )
L-Glutamine	3.81	NA <sup>c</sup>	WMCM (Weak <sup>d</sup> )
6-Phospho- gluconic acid	3.77	14.4 (0.2) <sup>a</sup>	WMCM (Weak <sup>d</sup> )
Pyruvic acid	3.66	3.6 (0.9) <sup>b</sup>	WMCM (Weak <sup>d</sup> )
Dihydroxyacetone phosphate	3.06	20 (1) <sup>a</sup>	WMCM (Weak <sup>d</sup> )

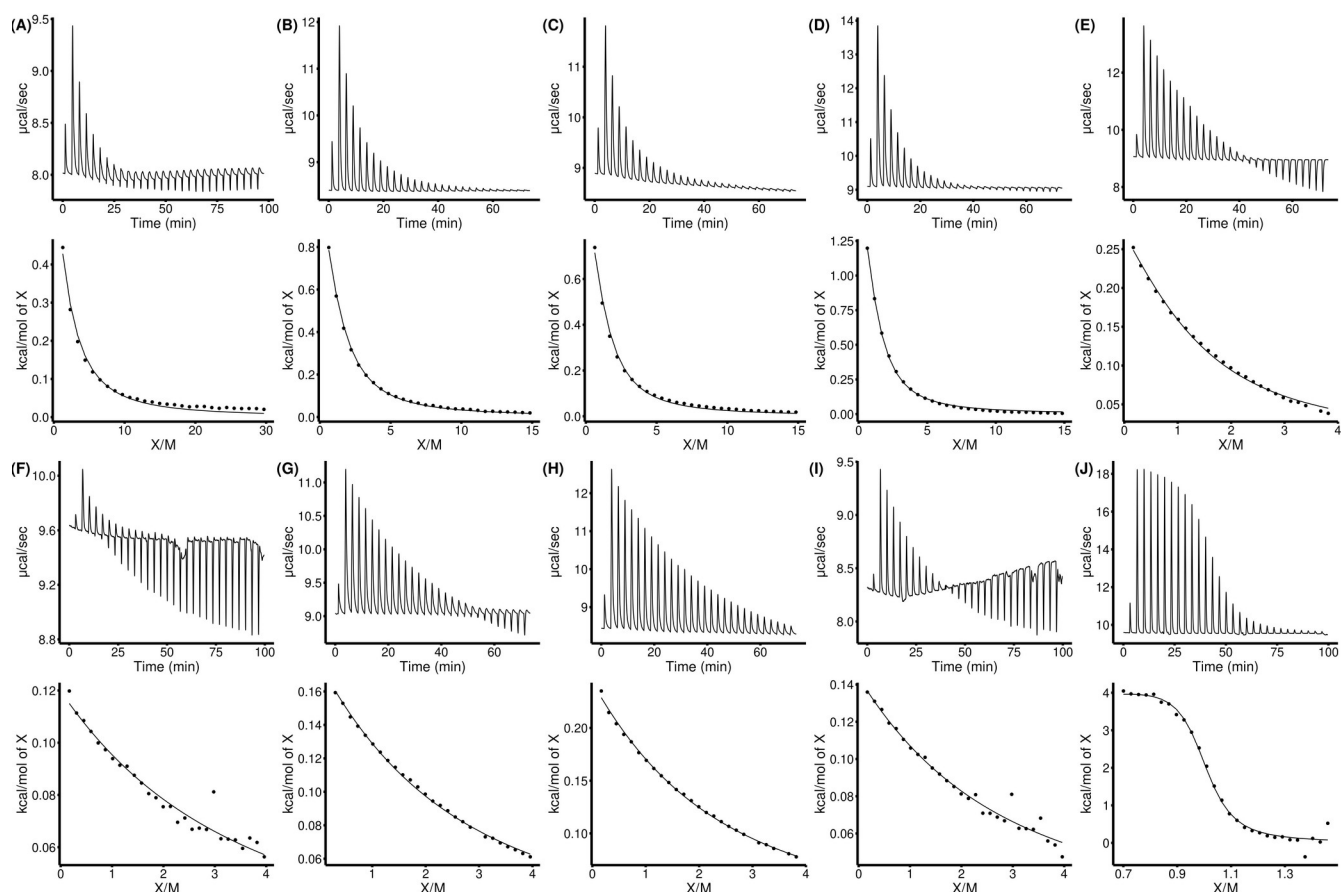
<sup>a</sup>Determined at 37 °C with Isothermal titration calorimetry. Error is the propagated standard error in the fit parameters.

<sup>b</sup>Determined at 37 °C with HQS emission Error is the propagated standard error in the fit parameters.

<sup>c</sup>No binding observed as per SI Figure 2

<sup>d</sup>Metabolites with K<sub>D</sub>s for Mg<sup>2+</sup> less than 2 mM are considered strong Mg<sup>2+</sup> chelators.

**SI Table 1.** Recipe for the Eco80 artificial cytoplasm (Add in later in word when I am formatting the tables)



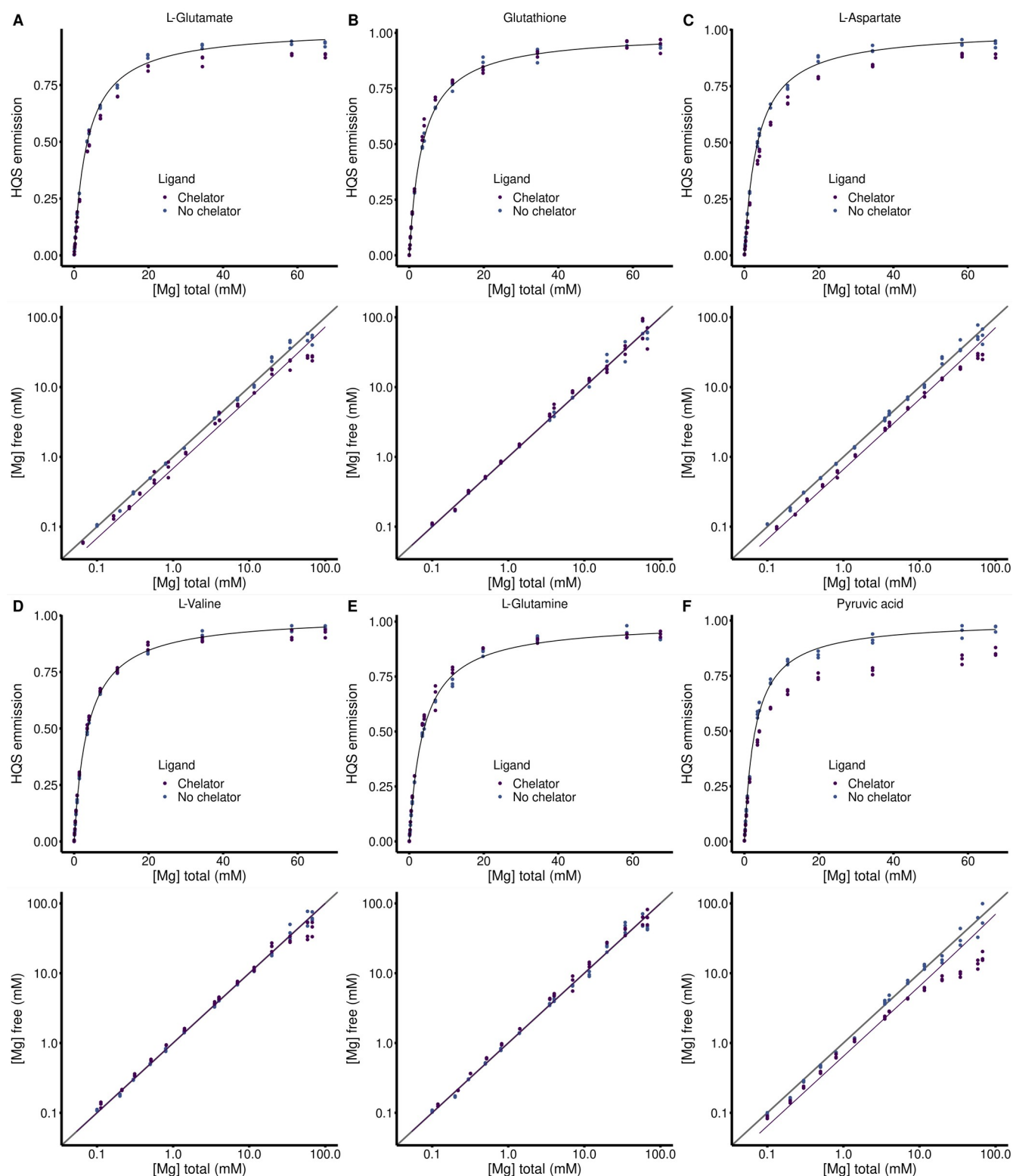
**SI Figure 1** Isothermal titration calorimetry (ITC) analysis of  $\text{Mg}^{2+}$  binding to metabolites in 240 mM NaCl 140 mM KCl 10 mM HEPES pH 7.0 at 37 °C.  $\text{MgCl}_2$  was titrated into metabolites and the power was monitored over time (Top panel). Heat of the injection was calculated by integrating the raw power curve, and the background heat of  $\text{MgCl}_2$  dilution, collected on buffer containing no metabolite, was subtracted to produce the isotherms in the bottom panels. Lines in bottom panels represent fits to the Weismann isotherm equation to determine apparent association constants. **(A)** Adenosine triphosphate (ATP). **(B)** Uridine triphosphosphate (UTP). **(C)** Guanosine triphosphate (GTP). **(D)** deoxythymidine triphosphate (dTTP). **(E)** Fructose 1,6-bisphosphate. **(F)** Uridine diphosphate (UDP)-N-acetylglucosamine. **(G)** Glucose 6-phosphate. **(H)** 6-phosphogluconic acid. **(I)** phosphoenol pyruvate. **(J)** Ethylene diamine-tetracetic acid (EDTA).

**SI Table 2** Apparent binding constants determined with Isothermal titration calorimetry (ITC).

Metabolite	Syringe (mM)	Cell (mM)	dH (kcal/mol)	K' (M <sup>-1</sup> )	K <sub>D</sub> ' (mM <sup>-1</sup> )
ATP	15 mM MgCl <sub>2</sub> <sup>a</sup>	0.1 mM ATP <sup>a</sup>	1.83 (0.04)	3600 (200)	0.28 (0.01)
UTP	15 mM MgCl <sub>2</sub> <sup>a</sup>	0.2 mM UTP <sup>a</sup>	1.70 (0.01)	4200 (70)	0.248 (0.004)
GTP	15 mM MgCl <sub>2</sub> <sup>a</sup>	0.2 mM GTP <sup>a</sup>	1.43 (0.02)	5000 (200)	0.201 (0.007)
dTTP	15 mM MgCl <sub>2</sub> <sup>a</sup>	0.2 mM dTTP <sup>a</sup>	2.19 (0.02)	6300 (300)	0.160 (0.003)
Fructose 1,6-BP	100 mM MgCl <sub>2</sub> <sup>a</sup>	5.0 mM Fructose 1,6- BP <sup>a</sup>	0.414 (0.004)	169 (4)	5.9 (0.1)
UDP-GlcNAC	100 mM MgCl <sub>2</sub> <sup>a</sup>	5.0 mM UDP- GlcNAC	0.57 (0.02)	34 (2)	29 (2)
Glucose 6-P	100 mM MgCl <sub>2</sub> <sup>a</sup>	5.0 mM Glucose 6-P <sup>a</sup>	0.555 (0.003)	57.9 (0.7)	17.3 (0.2)
6-P-gluconic acid	100 mM MgCl <sub>2</sub> <sup>a</sup>	5.0 mM 6-P- gluconic acid <sup>a</sup>	0.662 (0.005)	70 (1)	14.4 (0.2)
Dihydroxyacetone phosphate	100 mM MgCl <sub>2</sub> <sup>a</sup>	5.0 mM dihydroxy- acetone phosphate <sup>a</sup>	0.50 (0.01)	51 (3)	20 (1)
EDTA	6 mM MgCl <sub>2</sub> <sup>a</sup>	1.5 mM EDTA 1.0 mM MgCl <sub>2</sub> <sup>a,b</sup>	2.85 (0.04)	220,000 (30,000)	0.0045 (0.0006)

<sup>a</sup>240 mM NaCl 140 mM KCl 10 mM HEPES pH 7.0 at 37 °C

<sup>b</sup>Mg<sup>2+</sup> and EDTA were incorporated into the cell in order to sequester trace tight binding metal ions and thereby negate their contribution to ITC signal.



**SI Figure 2** HQS analysis of  $\text{Mg}^{2+}$  binding to metabolites in 240 mM NaCl 140 mM KCl 20 mM MOPS 0.01 mM EDTA 0.001% SDS pH 7.0. (Top panels) Dependence of HQS emission on the total concentration of  $\text{MgCl}_2$  in the presence and absence of a metabolite chelators. Black lines represent a fit to SI equation 1 to determine the  $F_{\max}$ ,  $F_{\min}$ , and  $K_{\text{HQS}}$ . (Bottom panels) Dependence of the free  $\text{Mg}^{2+}$  concentration on the total concentration of  $\text{MgCl}_2$  in the presence and absence of a metabolite chelators. Grey lines represent where the free  $\text{Mg}^{2+}$  concentration equals the total concentration of  $\text{MgCl}_2$ , Purple lines represent a fit to SI equation 4 to determine the association constant between HQS and a chelator. **(A)**

240 mM L-glutamate. **(B)** 194 Glutathione. **(C)** 240 mM L-aspartate. **(D)** 240 mM L-valine. **(E)** 240 mM L-glutamine. **(F)** 5 mM pyruvic acid.

**SI Table 3** Apparent binding constants determined with HQS emission.  $F_{\max}$ ,  $F_{\min}$ , and  $K_{\text{HQS}}$  are determined by fitting HQS emission in the absence of chelators and used to calculate the free  $\text{Mg}^{2+}$  concentration in each sample. Metabolite binding constants,  $K'$  and  $K_D'$ , are determined by fitting the relationship between the free  $\text{Mg}^{2+}$  concentration and the total  $\text{MgCl}_2$  concentration using SI Equation 4.

Metabolite	$F_{\max}$	$F_{\min}$	$K_{\text{HQS}}$ ( $\text{mM}^{-1}$ )	$K'$ ( $\text{mM}^{-1}$ )	$K_D'$ ( $\text{mM}^{-1}$ )
L-Glutamic acid	187,000 (1000)	0 (810)	0.281 (0.008)	0.0019 (0.0002)	520 (50)
Glutathione	182,000 (1000)	592 (750)	0.279 (0.007)	NA <sup>c</sup>	NA <sup>c</sup>
L-Aspartic acid	196,000 (1000)	0 (820)	0.283 (0.007)	0.0021 (0.0001)	465 (12)
L-Valine	188,200 (800)	495 (580)	0.274 (0.005)	NA <sup>c</sup>	NA <sup>c</sup>
L-Glutamine	190,000 (1400)	516 (110)	0.27 (0.01)	NA <sup>c</sup>	NA <sup>c</sup>
Pyruvic acid	188,000 (1500)	0 (1300)	0.35 (0.01)	0.28 (0.07)	3.6 (0.9)

<sup>c</sup>No binding observed as per SI Figure 2

**SI Table 3.** HQS fits in the absence of chelators, used to determine free  $\text{Mg}^{2+}$  concentrations.  $F_{\max}$ ,  $F_{\min}$ , and  $K_{\text{HQS}}$  are determined by fitting HQS emission in the absence of chelators and used to calculate the free  $\text{Mg}^{2+}$  concentration in each sample.

Metabolite	$F_{\max}$	$F_{\min}$	$K_{\text{HQS}}$ ( $\text{mM}^{-1}$ )
Eco80	185,100 (800)	124 (1000)	0.239 (0.005)
NTPCM	187,000 (1500)	436 (1000)	0.26 (0.01)
WMCM	179,000 (1600)	0 (1400)	0.32 (0.01)

**Table 2.** Total  $\text{Mg}^{2+}$  concentrations used to obtain 2 mM free  $\text{Mg}^{2+}$  in artificial cytoplasm.

Condition	Total [ $\text{Mg}^{2+}$ ] (mM)	Chelated [ $\text{Mg}^{2+}$ ] (mM)	Free [ $\text{Mg}^{2+}$ ] (mM)
Eco80	31.6	29.6	2.0
NTPCM	25.0	23	2.0
WMCM	6.4	4.5	2.0

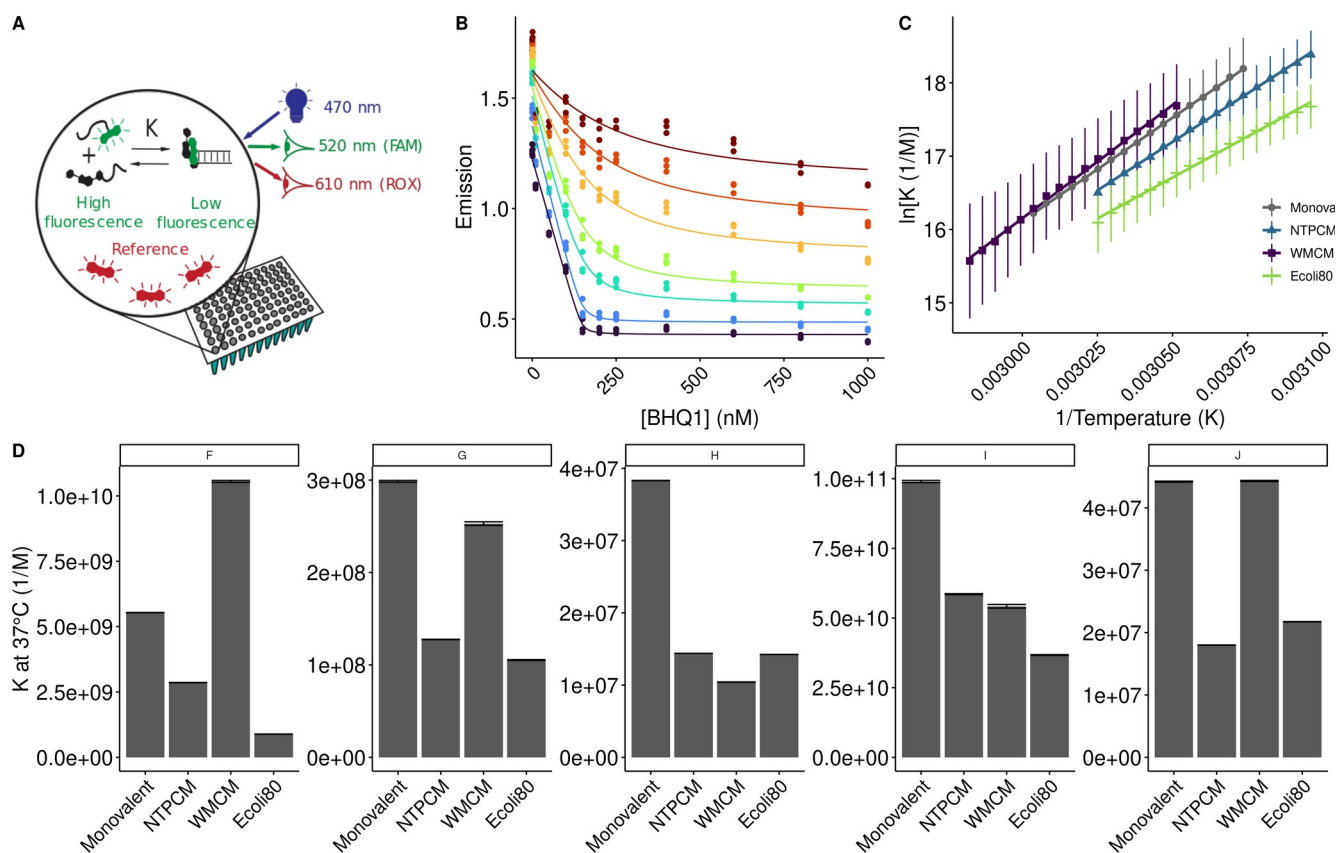
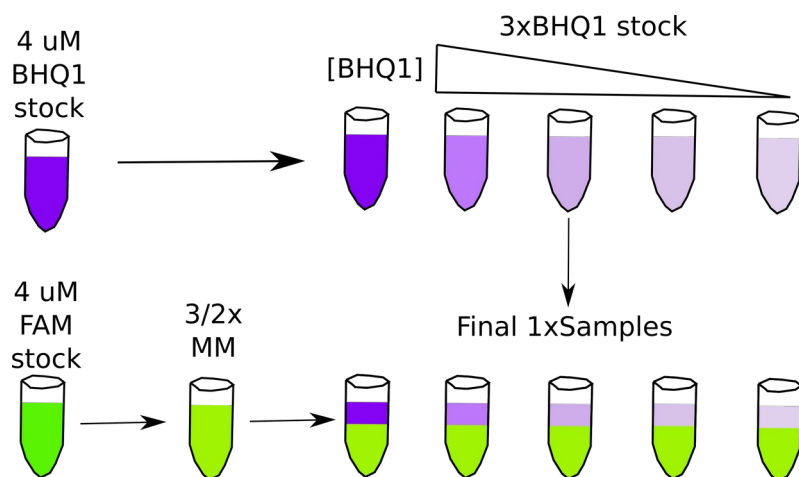
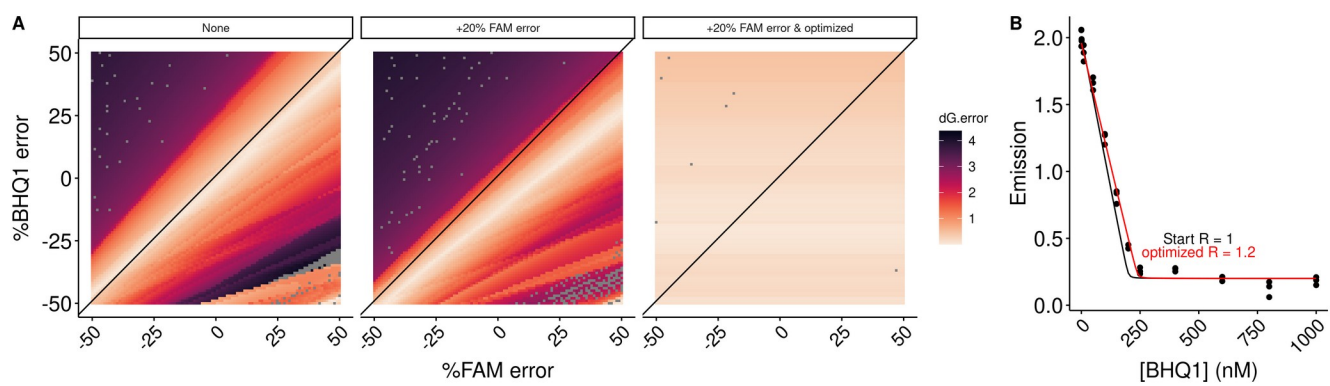


**Figure 2** *E. coli* metabolite and  $Mg^{2+}$  mixtures destabilize RNA secondary structure.



**SI figure 3** *E. coli* metabolite and  $Mg^{2+}$  mixtures destabilize RNA secondary structure.



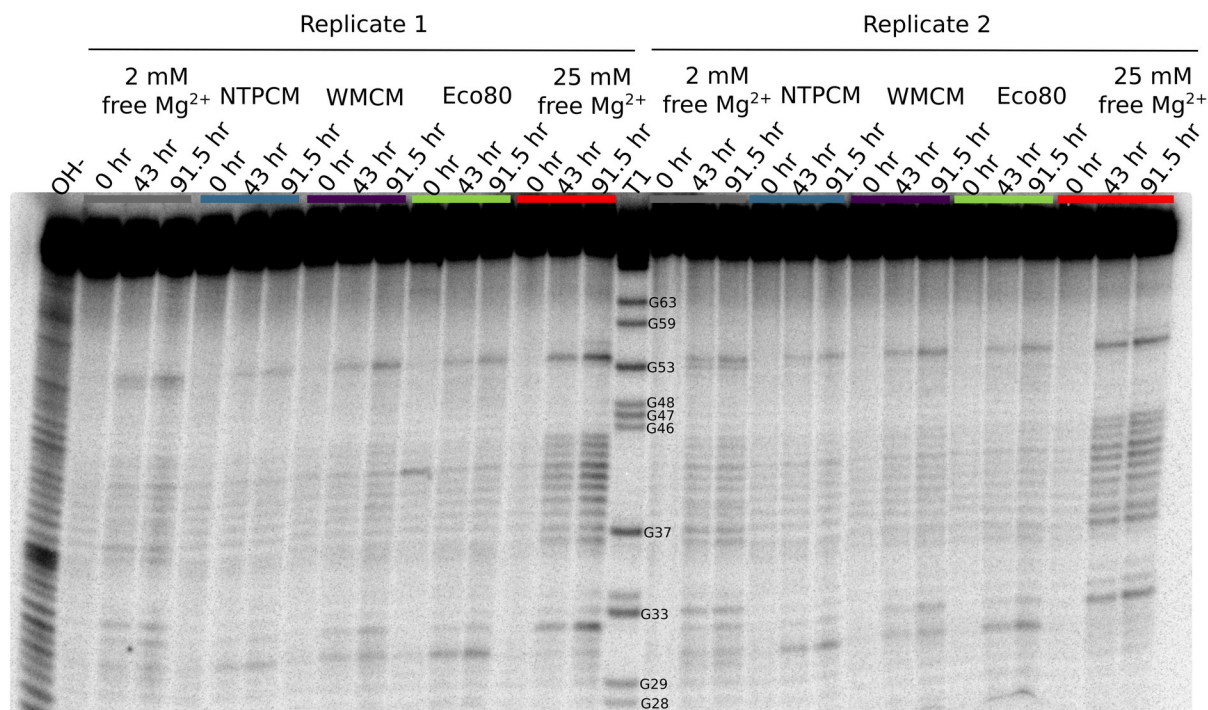


**SI figure 4** *E. coli* metabolite and  $\text{Mg}^{2+}$  mixtures destabilize RNA secondary structure.

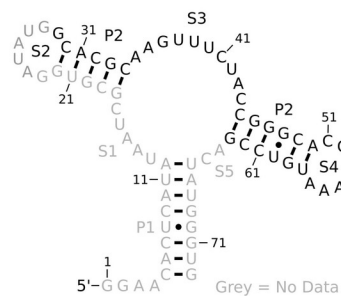
**Table 3. Stability of RNA helices in *E. coli* metabolite mixtures.**

Helix	Sequence (5'-FAM/ BHQ1-3')	AU content	Condition	dH (kcal/mol)	dS (cal/mol/K)	dG (kcal/mol)	ddG (kcal/mol)
F	CGCAUCCU/ AGGAUGCG	0.38	2 mM free	-55.9 (0.2)	-136.0 (0.7)	-13.82 (0.01)	
			NTPCM	-52.2 (0.4)	-125 (1)	-13.41 (0.02)	0.41 (0.02)
			WMCM	-61.4 (0.8)	-152 (2)	-14.22 (0.05)	-0.40 (0.05)
			Ecoli80	-44.5 (0.7)	-102 (2)	-12.70 (0.04)	1.13 (0.04)
G	CCAUAUCA/ UGAUAUGG	0.63	2 mM free	-53.4 (1.0)	-133 (3)	-12.02 (0.04)	
			NTPCM	-42.9 (0.5)	-101 (1)	-11.50 (0.02)	0.52 (0.04)
			WMCM	-53 (2)	-132 (7)	-11.9 (0.1)	0.10 (0.01)
			Ecoli80	-57 (2)	-146 (5)	-11.38 (0.05)	0.64 (0.06)
H	CCAUAUUA/ UAAUAUGG	0.75	2 mM free	-53.5 (0.4)	-137 (1)	-10.76 (0.01)	
			NTPCM	-45.0 (0.2)	-112.5 (0.5)	-10.158 (0.002)	0.60 (0.01)
			WMCM	-43 (2)	-107 (5)	-9.94 (0.02)	0.80 (0.02)
			Ecoli80	-41.3 (0.2)	-100.4 (0.7)	-10.15 (0.01)	0.61 (0.01)
I	CGGAUGGC/ GCCAUCCG	0.25	2 mM free	-71.1 (0.8)	-179 (2)	-15.6 (0.06)	
			NTPCM	-70.4 (0.6)	-177 (2)	-15.28 (0.05)	0.32 (0.08)
			WMCM	-65.5 (2)	-162 (7)	-15.2 (0.2)	0.4 (0.2)
			Ecoli80	-69.7 (0.8)	-176 (3)	-14.0 (0.1)	0.61 (0.08)
J	CGUAUGUA/ UACAUACG	0.63	2 mM free	-63.2 (0.9)	-169 (3)	-10.85 (0.02)	
			NTPCM	-59 (1)	-157 (4)	-10.30 (0.01)	0.55 (0.02)
			WMCM	-67 (1)	-180 (3)	-10.85 (0.02)	0.00 (0.03)
			Ecoli80	-61 (1)	-164 (3)	-10.41 (0.01)	0.44 (0.02)

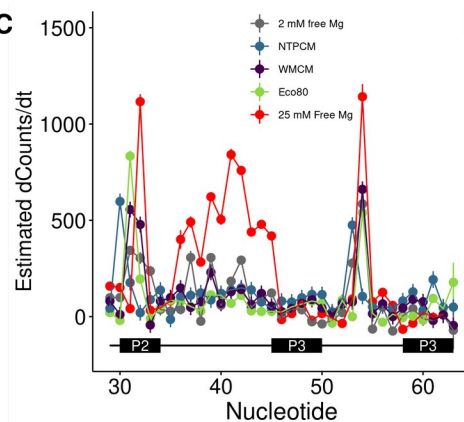
**A**



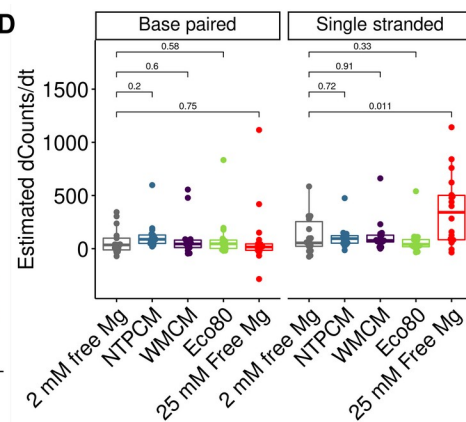
**B**



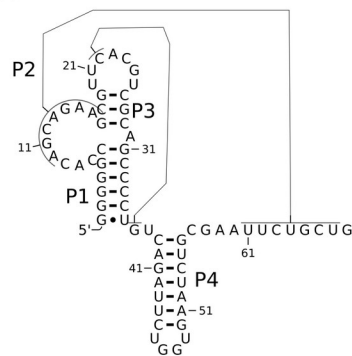
**C**



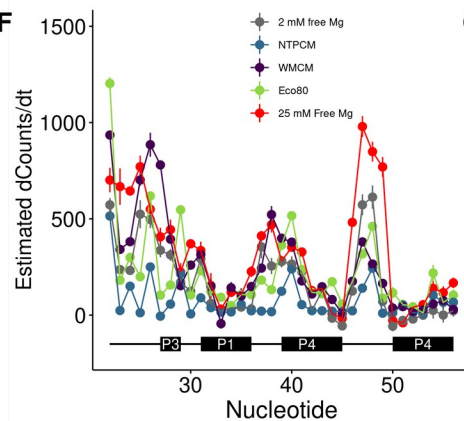
**D**



**E**



**F**



**G**

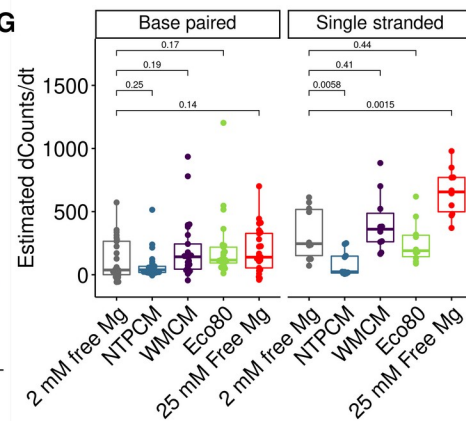


**Figure 3** *E. coli* metabolite and  $Mg^{2+}$  mixtures stabilize the chemical structure of RNA. **(A)** Raw degradation assay gel image for the Guanine riboswitch aptamer incubated in artificial cytoplasms at 37 °C and pH 7. The OH- lane contains a hydrolysis ladder which cleaves after every nucleotide and T1 contains the RNA treated with T1 ribonuclease which cleaves after every G. Enough  $Mg^{2+}$  was added to each artificial cytoplasm to have 2 mM  $Mg^{2+}$  as determined in Figure 1. **(B)** Secondary structure of the guanine riboswitch aptamer. **(C)** Estimated increase in counts as a function of time at each residue in different solution conditions as a function of location in the RNA. **(D)** Estimated increase in counts as a function of time in different conditions grouped by paired and unpaired bases. Significance was determined using a student's t-test. **(E)** Secondary structure of the cleaved human CPEB3 HDV ribozyme. **(C)** Estimated increase in counts as a function of time at each residue in different solution conditions as a function of location in the RNA. **(D)** Estimated increase in counts as a function of time in different conditions grouped by paired and unpaired bases. Significance was determined using a student's t-test.

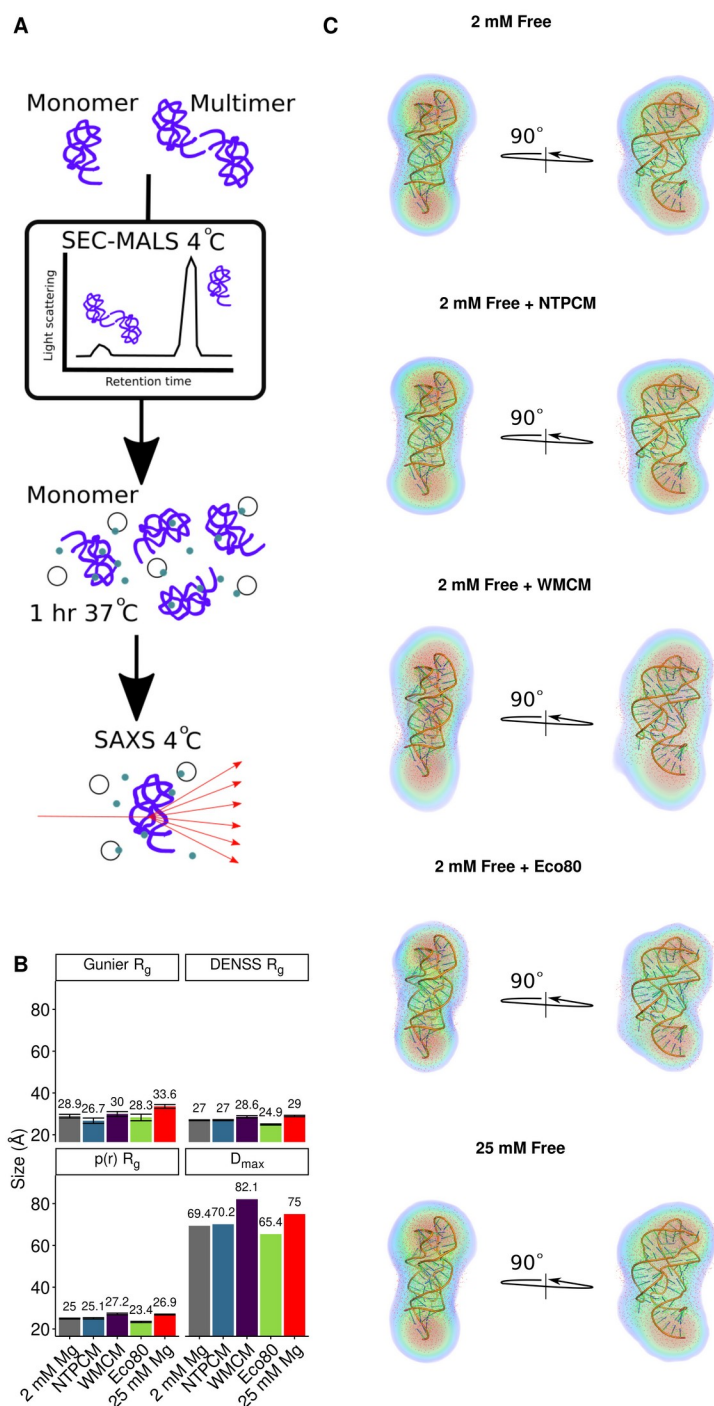


**Figure 4** *E. coli* metabolite and  $Mg^{2+}$  mixtures increase functional RNA compactness.